J. Fluid Mech. (1980), *vol.* **99**, *part* 2, *pp.* 247–265
Printed in Great Britain

Nonlinear evolution and breakdown in unstable boundary layers

By A. D. D. CRAIK
Department of Applied Mathematics, University of St Andrews, Fife KY16 9SS

(Received 28 December 1978 and in revised form 25 October 1979)

The nonlinear evolution and breakdown of laminar flow in the boundary layer on a flat plate is examined with the aim of making a closer comparison of theory and experiment than has been attempted previously. The importance of three-dimensionality is emphasized. It is concluded that many features of the nonlinear instability are consistent with existing linear and weakly nonlinear theories even as breakdown is approached. The development of the secondary instability, or 'spike', is also considered and suggestions for an improved theory of its growth are made.

1. Introduction

Beginning his review of boundary-layer transition, Tani (1969) remarks that 'The problem of the transition from laminar to turbulent flow in the boundary layer is unparalleled in having attracted the interest of investigators for so many years. Despite the enormous amount of research effort devoted to it, our understanding of the problem is still far from complete.' Ten years on, this situation has not greatly changed, although the research effort continues and some important advances have been made.

The aim of this paper is to provide a closer comparison of theory and experiment than has been attempted previously. In so doing, a clearer view emerges of the areas of agreement and of uncertainty, and a better appreciation is reached of the extent to which weakly nonlinear theories can provide a satisfactory interpretation of the observational evidence. The experiments discussed are mainly those of Klebanoff, Tidstrom & Sargent (1962) and of Kovasznay, Komoda & Vasudeva (1962). Various theoretical models will be referred to.

It must first be emphasized that these admirable experiments do not map the *only* pathway from laminar to turbulent flow. In 'real-life' flows, surface roughness, free-stream turbulence and several other factors may alter or bypass the Tollmien–Schlichting instability mechanism (see, for instance, Tani's (1969), Reshotko's (1976) and Morkovin's (1978) reviews). Furthermore, in a controlled experimental situation, the process to transition will depend on the nature of the disturbances which are deliberately introduced into the flow. The vibrating ribbon of Klebanoff *et al.* (1962) imposed a particular class of disturbances, characterized by a single frequency and slight spanwise variations. The sequence of events may be significantly different for other types of disturbance; for instance those with two or more frequencies (Kachanov, Kozlov & Levchenko 1978) or substantial spanwise variations in boundary-layer thickness (Komoda 1967), or for a spatially localized 'packet' (Gaster & Grant 1975; Wygnanski, Haritonidis & Kaplan 1979).

0022–1120/80/4481–1340 $02.00

The linear stability of a single two-dimensional Tollmien–Schlichting wave in Blasius flow has been extensively studied. There is good agreement between theory and the classic experiments of Schubauer & Skramstad (1948) and also the more recent ones of Ross *et al.* (1970). In addition, Gaster & Grant (1975) and Gaster (1975) find close agreement between linear theory and experiment for the initial development of a localized disturbance.

Mack (1977, 1978) has calculated the spatial linear amplification rate and associated complex group velocity of two-dimensional and oblique wave modes. The eigenvalue spectrum of the Orr–Sommerfeld equation with Blasius flow has been investigated by Jordinson (1971), Corner, Houston & Ross (1976) and Mack (1976); while systematic extension of linear theory to account for boundary-layer growth with downstream distance has been undertaken by Bouthier (1972, 1973), Gaster (1974) and Saric & Nayfeh (1975). Numerical solutions of the full Navier–Stokes equations for small-amplitude disturbances by Fasel (1976) show good agreement with the Orr–Sommerfeld results. Murdock's (1977) computations show similar agreement at small amplitude, and deal also with larger two-dimensional disturbances for which the influence of nonlinearity is evident; while Orszag (1976) considers finite-amplitude three-dimensional disturbances.

It is clear that, as computational techniques improve, 'numerical experiments' based on the full Navier–Stokes equations will increasingly complement physical experiments and theoretical models based on linear and weakly nonlinear approximations. Agreement of linear theory, experiment and small-amplitude computer solutions of the Navier–Stokes equations is gratifyingly good. In contrast, existing comparisons of *nonlinear* theories and computations with experiments are sketchy, revealing qualitative rather than quantitative similarities.

Notable among the weakly nonlinear theories stemming from the seminal paper of Landau (1944) is the work of Stuart (1960) and Watson (1960) and the well-known Benney–Lin theory (Benney & Lin 1960; Benney 1961, 1964; see also Antar & Collins 1975; Nelson & Craik 1977). The former concerns two-dimensional waves only, and extensions of this work to the Blasius boundary layer have been attempted by Itoh (1974) and Herbert (1975). Other recent work by Itoh (1977) and, especially, Herbert (1977) give hope of further progress in this area. However, the present paper is primarily concerned with three-dimensional disturbances.

The analyses of Benney and Lin yield a plausible explanation of the developing three-dimensional 'longitudinal-vortex' structure of the mean flow. In addition, the mutual interaction of two- and three-dimensional wave modes has been examined by Stuart (1962), Craik (1971) and Usher & Craik (1975). These studies together reveal a wealth of theoretical possibilities, all of which seem to favour the growth of three-dimensionality in one way or another, but the details are quite different. The three-wave resonance envisaged by Craik (cf. the early work of Raetz 1959) involves second-order interactions among waves with two frequencies, one half of the other; Usher & Craik extended this work to include third-order terms and also considered non-resonant cases with the same wavenumber configuration; Stuart investigated third-order interactions among two- and three-dimensional waves with the same downstream wavenumbers. If these analyses are correct, then suitably controlled experiments should display the features which they predict. As close a comparison as possible should therefore be made with the existing experimental data, both to help interpret

that data properly and to provide a check on the relevance of the theoretical models for these experiments.

Here such a comparison is attempted with the observations of Klebanoff *et al.* and Kovasznay *et al.* In many respects, the two sets of experiments are similar. Accordingly, comparisons are mainly made with the former, except where the latter reveal additional features. Some of the work described here is also reported briefly in Craik (1979).

Other, visual studies of similar configurations, notably by Hama & Nutant (1963) and Wortmann (1977), are also of undoubted interest. But these are less amenable to direct comparison with existing theories and are therefore not discussed in such detail here. Likewise, the interesting work of Kachanov, Kozlov & Levchenko (1977, 1978) and that of Saric & Reynolds (1979), which emphasizes the spectral composition of the disturbances, is considered only briefly.

2. Comparison with the linear eigensolutions

The data of Klebanoff *et al.* on 'controlled' transition concern input disturbances of a single frequency, supplied by a vibrating ribbon. As these disturbances propagate downstream and amplify, marked spanwise variations in amplitude appear, with a spanwise wavelength of 1 inch equal to the spacing of 0·003 inch thick cellophane strips placed on the plate beneath the vibrating ribbon. (These strips were introduced to control the three-dimensionality after earlier attempts to eliminate it had proved unsuccessful). Second and third harmonics of this fundamental frequency are later detected, but these remain fairly small; the second harmonic only approaching 20 % of the fundamental, and the third harmonic 8%, at a 'peak' station (i.e. at spanwise positions of maximum amplitude) as breakdown to turbulence is approached. Since no evidence of *sub*harmonics is reported, it would appear that the growth of three-dimensional disturbances cannot here be due to a resonant triad interaction between the fundamental two-dimensional wave and two oblique waves with half the frequency. However, it should be noted that subharmonics *were* detected by Kachanov *et al.* (1977, 1978), though these were absent in the similar experiment of Saric & Reynolds (1979).

While the Benney–Lin mechanism provides a model for the generation of a spanwise-periodic *mean* flow distortion similar to that observed experimentally, it does not describe how the initial almost two-dimensional waves develop a strong spanwise periodicity. The original Benney–Lin model may be thought of as comprising three plane waves of equal downstream wavenumber α, one of which is independent of spanwise distance z and the other two having equal and opposite spanwise wavenumbers $\pm\beta$. Regarding the amplitudes of these waves as being $O(\epsilon)$, the quadratic interaction of the two-dimensional and spanwise-varying waves drives a system of $O(\epsilon^2)$ longitudinal eddies with spanwise wavenumber β and zero frequency provided – as they assumed – all three waves have the same frequency. Further, the quadratic interaction of the two spanwise-varying waves leads to an $O(\epsilon^2)$ longitudinal vortex structure with wavenumber 2β. There is some experimental evidence of such wavenumber doubling (Klebanoff *et al.* 1962, figure 19). However, it was pointed out by Stuart (1962) that wavenumbers corresponding to the experimental configuration have linear frequencies which differ by about 15 %, contrary to the constant-frequency assumption of Benney & Lin.

Any synchronization of wave frequencies by nonlinear effects must take place, if at all, at a higher order of the perturbation analysis than that developed by Benney & Lin: in this respect, their analysis is deficient. One possibility is to retain a frequency mismatch $\Delta\omega$ in the second-order theory, as done by Antar & Collins (1975); in which case the mean flow distortion with wavenumber β oscillates with frequency $\Delta\omega$ but that with wavenumber 2β has zero frequency. A second alternative is to introduce a mismatch $\Delta\alpha$ in the downstream wavenumber of such a magnitude as to ensure that the waves have identical frequencies at linear approximation. This causes the mean flow distortions to have x and z wavenumber components $(\Delta\alpha, \beta)$ and $(0, 2\beta)$ respectively. Such a model was studied by Nelson & Craik (1977), with additional simplifying but restrictive assumptions which enabled analytic solutions to be obtained. A third possible theoretical development is to suppose that the waves *are* of equal or nearly equal frequency and downstream wavenumber and to carry the analysis to third order in wave amplitudes in order to derive the (truncated) nonlinear evolution equations for the wave amplitudes, which will determine *a posteriori* whether such nonlinear synchronization is feasible.

Third-order synchronization seems a more attractive proposition than the second-order frequency- or wavenumber-mismatch models, since no such fluctuations of the longitudinal vortex structure, either in time or in space, are reported by Klebanoff *et al.* However, it can be argued that their observations did not cover a sufficient region to detect a small downstream wavenumber $\Delta\alpha$. That wavenumber is about 15 % of the fundamental wavenumber α (corresponding to experimental downstream and spanwise wavelengths of 1·5 in and 1 in respectively) and so a downstream distance of several inches should have revealed its presence, if it existed. The published experimental data cover a distance of under 4 inches between their stations B and D, but the measurements at D are much distorted by the growing 2β-wavenumber component (see figure 18 of Klebanoff *et al.* 1962). The data is therefore inconclusive on this point. The two primary flows studied by Benney (1961, 1964) had piecewise-linear and tanh y velocity profiles, and so cannot be expected to yield secondary flows which agree closely with those for the experimental Blasius profile. But Antar & Collins (1975) investigated several Falkner–Skan profiles, including Blasius flow, retaining the frequency mismatch between waves, and their results seem to agree better with the experimental details. Of particular interest is the vertical (i.e. normal to plate) structure of the mean secondary flow. Benney's (1961) work predicts an array of counter-rotating eddies, one set above and another below the critical layer; but no set of eddies was detected below the critical layer by Klebanoff *et al.*, who speculate that it may be suppressed by the presence of the wall (cf. Benney 1964), and also point out that reliable measurements close to the wall are difficult to obtain. Antar & Collins obtain solutions both with and without the second set of 'wall eddies', depending on their choice of parameters.

It should be realized that the developing three-dimensional wave structure is also sensitive to pre-existing spanwise variations of the mean flow, whether inadvertent (Klebanoff & Tidstrom 1959) or deliberate (Komoda 1967). It is known that such mean-flow variations, once present, are remarkably persistent (see Crow 1966; Joseph & Hung 1971). The Benney–Lin theory considers that variations $O(\epsilon^2)$ in mean flow occur in response to the nonlinear interaction of two $O(\epsilon)$ wave modes; but an alternative and complementary theoretical model can be constructed in which an $O(\epsilon)$

two-dimensional wave and an $O(\epsilon)$ spanwise-varying mean-flow modification may interact to generate oblique wave modes. A similar problem has recently been tackled by Nayfeh (1979). It is arguable that some of the experimental data may correspond more closely to the latter than to the former model. (I am grateful to Prof. M. Morkovin for emphasizing this point to me.) In such a model, the question of synchronization of frequencies of two- and three-dimensional modes must again necessarily arise.

There is a further theoretical difficulty associated with the downstream growth of the boundary layer. As the waves progress downstream, their local wavenumber, growth rate and mode structure must alter in response to the varying boundary-layer profile. Such evolution, according to *linear* theory, has been convincingly studied (see above); but efforts to incorporate these effects into a consistent nonlinear theory have not proved entirely satisfactory (see Itoh 1974; Herbert 1975).

Klebanoff *et al.* (1962) conjectured that the developing spanwise variations in wave amplitude were a direct consequence of the local spanwise variations in Reynolds number caused by the spacers placed below the vibrating ribbon. A small increase in Reynolds number would therefore cause increased amplification of a wave with frequency close to branch I and decreased amplification of a frequency close to branch II of the Tollmien–Schlichting linear stability diagram. Their figure 13 certainly displays these features.

However, this suggestion has an obviously rational theoretical justification only for a predominantly two-dimensional wave with amplitude modulation on a spanwise length scale which is long compared with the fundamental wavelength. The actual disturbances have a spanwise wavelength of 1 in., which is similar in magnitude to the downstream wavelength (1·5 in. for a 145 Hz wave and greater for a 65 Hz wave). Accordingly, the disturbances are inherently three-dimensional and the proposed explanation of Klebanoff *et al.*, based on two-dimensional arguments, is an oversimplification. Further theoretical work on the stability of spanwise-varying flows is necessary in order to model this situation: at present, a full theoretical explanation of Klebanoff *et al.*'s (1962) figure 13 is lacking.

The vibrating ribbon produces disturbances of a single frequency ω which are predominantly two-dimensional. But the initially small three-dimensional ingredients must consist largely of waves with spanwise wavelength equal to 1 in. Such waves, with x, y, t periodicities of the form $B^{\pm}\exp i(\alpha_1 x \pm \beta y - \omega t)$ and spatially varying amplitudes $B^{\pm}$ should – according to linear theory – have downstream wavenumber α_1 roughly 15% less than the wavenumber α of the two-dimensional wave of form $A\exp i(\alpha x - \omega t)$. To be more precise, if $2\pi/\alpha$ corresponds to a downstream wavelength of 1·5 in. as for Klebanoff *et al.*'s 145 Hz wave at $U_1/\nu = 3{\cdot}1 \times 10^5\ \mathrm{ft}^{-1}$, and if the three-dimensional waves have a spanwise wavelength of 1 in., then $\beta/\alpha = \frac{3}{2}$ and examination of curves of constant frequency in the two-dimensional α, β wavenumber space (as shown for instance in figure 2 of Craik (1971) shows that $\alpha_1/\alpha \simeq 0{\cdot}85$. This implies that the wavenumbers $(\alpha_1, \pm\beta)$ correspond to plane waves $B^{\pm}$ propagating at equal and opposite angles of nearly 60° to the flow direction.

Of course, $|B^+| = |B^-|$ for symmetry, ensuring that the wave pattern has a standing rather than propagating spanwise variation. At propagation angles of 60°, the effective Reynolds number is reduced by half, in accordance with Squire's transformation, and such waves may be *damped*, rather than amplified, according to linear theory. But

the damping will be sufficiently small for fairly weak nonlinear terms to cause these waves to grow, rather than decay, with distance downstream.

Klebanoff *et al.* supply details of the r.m.s. intensity u' of the downstream velocity fluctuation at various downstream and spanwise locations (see their figure 5). Also, the relative amplitudes of the two- and three-dimensional waves may be inferred from their figures 2 and 3. According to their figure 2, with a 145 Hz wave measured at 0·042 in from the plate and 3 inches downstream of the ribbon, u'/U_1 is approximately 0·008 and 0·012 at 'valley' and 'peak' spanwise positions respectively; at 6 inches downstream the corresponding values are about 0·006 and 0·030; and at 7·5 inches about 0·017 and 0·068 respectively. These readings imply u'/U_1 amplitudes of $|A| = 0{\cdot}010$, 0·018 and 0·042 for a two-dimensional wave at the three downstream positions, and corresponding oblique wave amplitudes of $|B^{\pm}| = 0{\cdot}001$, 0·006 and 0·013. (Note that the difference of the 'peak' and 'valley' values of u'/U_1 must equal $4|B^{\pm}|$.) The values are inconsistent with exponential growth of the waves, suggesting that the linear growth or decay rates are substantially modified by nonlinear effects. (However, downstream growth of the boundary layer must also produce departures from exponential amplification.)

Despite the undoubted presence of nonlinear effects, it does not follow that the local structure of the waves must depart substantially from that predicted by linear theory: indeed the central assumption of *weakly* nonlinear theory is that the wave eigenfunctions given by linear theory continue to yield good approximations to the structure of the wave motion, across the boundary layer. In particular, the structural changes with increasing wave amplitude (such as shown in Klebanoff *et al.*'s figure 5) are not necessarily evidence of 'strong' nonlinearity, as is often assumed. In fact, it is here shown that the experimental records agree quite well with the appropriate linear eigenfunctions, even up to station D, which is close to 'breakdown'.

It is important to recognize that the velocity perturbations associated with the oblique waves have *three* velocity components. The components normal to the plate and normal to the crests of a plane oblique wave are determined by the reduced two-dimensional problem, in accordance with Squire's theorem; the third component, that parallel to the wave crests, results from distortion by the vertical motion of the component of the mean flow directed along the wave crests. The total measured u' velocity in the x direction will comprise (i) the downstream component associated with the two-dimensional wave A, (ii) the downstream component of the velocities normal to the crests of the oblique waves $B^{\pm}$ and (iii) the downstream component of the velocities parallel to the crests of the oblique waves $B^{\pm}$.

A significant feature of ingredients (i) and (ii) is that the phase of these fluctuations remains almost constant with depth (except within a narrow layer across which it changes rapidly by almost π radians); this is readily confirmed from figure 1(*b*), which shows that the imaginary part of this velocity component greatly exceeds its real part throughout the boundary layer. In contrast, the phase of the velocity component (iii) shows marked variations with depth because its real and imaginary parts are functions of depth which are comparable in magnitude (see figure 1*a*). This component, denoted by $\hat{v}^{\pm}$ for the respective oblique waves, obeys a linearized equation of the form (cf. Craik 1971, §3)

$$\{i\alpha(\bar{u}-c)-R^{-1}(d^2/dy^2-\gamma^2)\}\hat{v}^{\pm} = \mp i\bar{u}'\beta\phi^{\pm}, \tag{2.1}$$

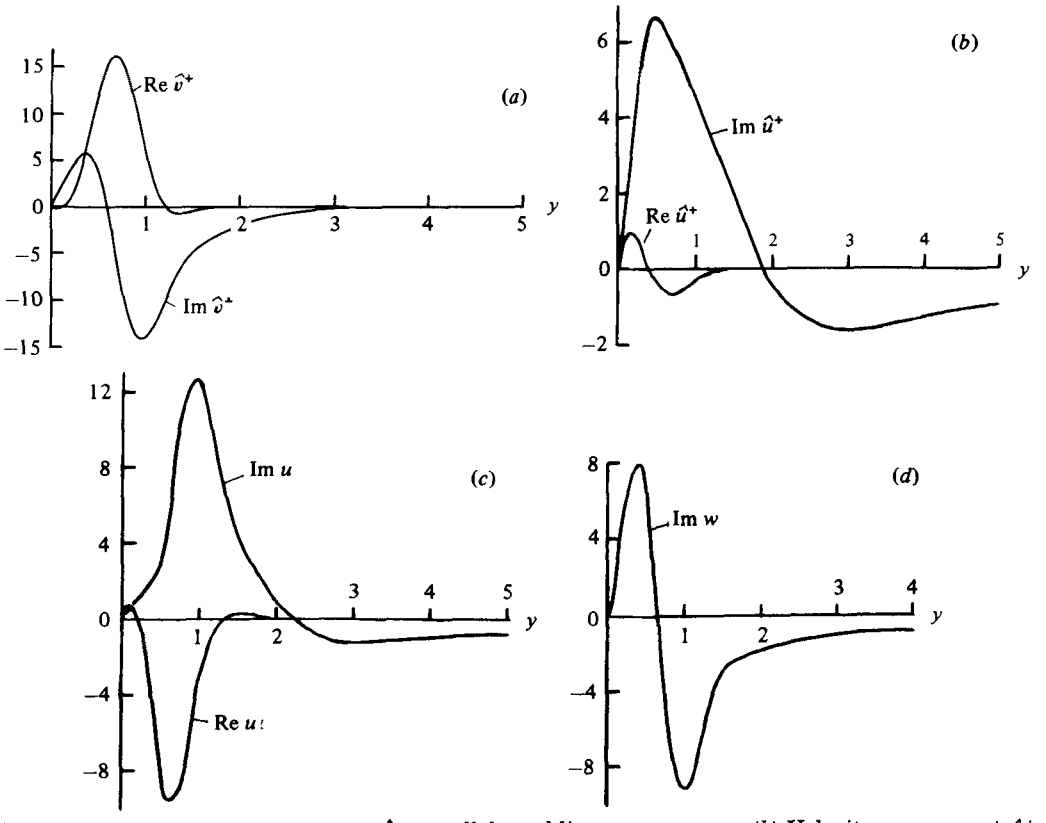

FIGURE 1. (*a*) Velocity component $\hat{v}^+$ parallel to oblique wavecrests. (*b*) Velocity component $\hat{u}^+$ normal to oblique wave crests. (*c*) Composite downstream velocity component

$$u = \gamma^{-1}(\alpha\hat{u}^+ - \beta\hat{v}^+).$$

(*d*) Imaginary part of composite spanwise component $w = \gamma^{-1}(\beta\hat{u}^+ + \alpha\hat{v}^+)$. Re w is virtually (α/γ) Re $(\hat{v}^+)$. Results due to Hendriks (see appendix to Usher & Craik 1975) for case $R = 882$, $\alpha = 0{\cdot}25$, $\beta = 0{\cdot}1991$, $\gamma = 0{\cdot}3145$ with propagation angle of 37·4°.

where $\bar{u}(y)$ is the primary flow, $c = c_r + ic_i$ is the complex phase velocity in the x direction, $\gamma^2 \equiv (\alpha^2+\beta^2)$ and $\phi^\pm$ is the appropriate eigenfunction of the reduced Orr–Sommerfeld problem. The appropriate boundary conditions are $\hat{v}^\pm(0) = 0$ and $\hat{v}^\pm \to 0$ as $y \to \infty$. The solution of this equation for the Blasius flow profile is given by F. Hendriks, in the appendix to the paper by Usher & Craik (1975), for $\alpha = 0{\cdot}25$, $\beta = 0{\cdot}1911$ and a Reynolds number based on displacement thickness of $R = 882$. (Note that in that paper $\frac{1}{2}\alpha$ corresponds to the present α for oblique waves. Also, the solution for negative β is just minus that for positive β.) This wave propagates at 37·4° to the x direction, which is considerably less than the 60° angle inferred from Klebanoff *et al.*'s data; but the structure of $\hat{v}^\pm$ is certain to be similar in the two cases. Hendrik's solution is reproduced here in figure 1(*a*). The y co-ordinate is defined so that the displacement thickness of the boundary layer is unity. There do not seem to be any other published solutions for this velocity component. Though Antar & Collins (1975) certainly also computed it, they do not describe their results.

Hendriks' result may be compared with the solution of the equation

$$\{i\alpha(y-c) - R^{-1}d^2/dy^2\}\,\hat{v}^\pm = \text{constant},$$

which may be renormalized as

$$(d^2/dY^2 - iY)\,\hat{v}^{\pm} = 1 \tag{2.2}$$

with $Y \equiv (\alpha R)^{\frac{1}{3}}(y-c)$ representing distance from the critical layer. The solution of the latter equation, with the boundary conditions $\hat{v}^{\pm} \to i/Y$ as $Y \to \pm\infty$, was first found by Holstein (1950) in connexion with the asymptotic viscous solutions of the Orr–Sommerfeld equation; and some properties of this function, now known as a Lommel function, are outlined by Benney (1961, 1964) and Craik (1971). Despite the closeness of the critical layer to the wall in Hendriks' case, the real and imaginary parts of his $\hat{v}^{\pm}$ display the same broadly symmetric and antisymmetric structure about the critical layer as the Lommel function.

Figure 1(*b*) shows the eigenfunction for the velocity component $\hat{u}^+$ normal to the wave crests and figure 1(*c*) shows the composite downstream velocity perturbation of the oblique wave, defined as $u = \gamma^{-1}(\alpha\hat{u}^+ - \beta\hat{v}^+)$, for Hendriks' case $R = 882$, $\alpha = 0{\cdot}25$, $\beta = 0{\cdot}1911$, $\gamma = 0{\cdot}3147$. Figures 1(*b*), (*c*) clearly show that the phase of $\hat{u}$ remains fairly constant across the boundary layer, apart from a sudden change of π at $y = 1{\cdot}85$ where Re $\hat{u}$ changes sign; but that the phase of the overall downstream velocity perturbation u changes continuously, owing to the $\hat{v}^+$ contribution. (Note that $y = 1{\cdot}85$ is *not* near the critical layer, which is at $y = 0{\cdot}67$.)

When a two-dimensional wave and a pair of oblique waves are present, as in the experiments considered, the phase variation of the total downstream velocity perturbation will resemble that of $\hat{u}$ when the two-dimensional wave is of much greater amplitude than the others; but, as the three-dimensional waves attain larger amplitudes, the phase will vary continuously, in a manner determined by the relative intensities and phases of the two- and three-dimensional components. This is in accord with figure 8 of Klebanoff *et al.*

The variations in root-mean-square intensity of the downstream velocity fluctuation shown in figure 5 of Klebanoff *et al.* may also be understood as the contributions from the three waves, *essentially as given by linear theory*. Such variations are here modelled in figure 2(*a*, *b*). To avoid further computations, it was supposed that the velocity associated with a two-dimensional wave is just $2\hat{u}(y)$ as shown in figure 1(*b*), and that the downstream velocity associated with the pair of oblique waves is

$$e^{i\theta}\,u(y)\cos\beta z,$$

where θ is a constant phase lag. This corresponds to oblique waves with amplitudes $\frac{1}{4}$ that of the two-dimensional wave. The r.m.s. fluctuations across the boundary layer are shown for $\cos\beta z = 1$, 0 and -1, the curves in figure 2(*a*) being for $\theta = 0$ and those in figure 2(*b*) for $\theta = \frac{1}{2}\pi$. It is clear that, for varying wave-amplitudes and phase lags, the distribution of intensity assumes differing shapes. The greatest intensity is recorded at $y = 0{\cdot}8$ for $\theta = 0$ and $\cos\beta z = 1$, while the maximum intensity for the two-dimensional wave alone is at $y = 0{\cdot}5$. This displacement of the peak of intensity away from the wall, and other general characteristics of the waves shown, are consistent with the experimental data of Klebanoff *et al.* It is possible that the presence of curves with double maxima at the experimental station B and the absence of such curves at station C indicate a change in phase θ of the three-dimensional wave pattern relative to the two-dimensional wave over this distance of just under 2 in. This provides some slight support for the view that the downstream wavenumbers of two- and three-dimensional waves must differ.

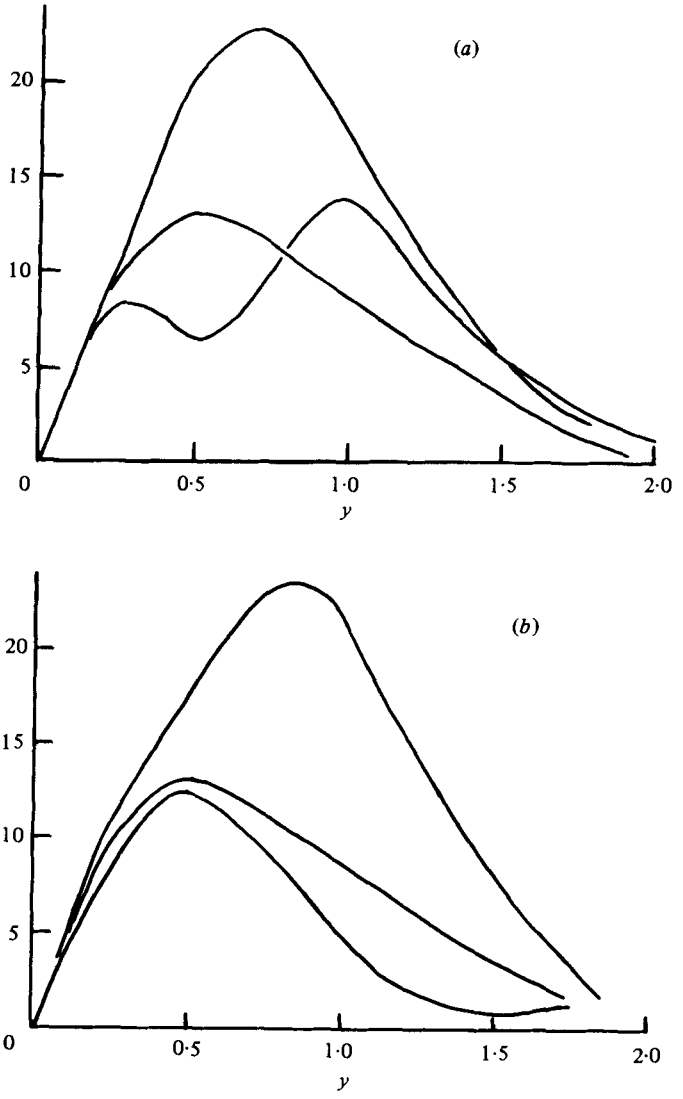

FIGURE 2. R.m.s. downstream velocity fluctuations across boundary layer for combination of two- and three-dimensional waves, at spanwise stations $\cos \beta z = 1$, 0 and -1. (*a*) Results for phase lag $\theta = 0$. (*b*) Results for phase lag $\theta = \frac{1}{2}\pi$.

The *instantaneous* u-velocity fluctuation across the boundary layer, given by $\mathrm{Re}\{u\, e^{i\omega t}\}$, also varies substantially both with time and with spanwise location. Figure 17 of Klebanoff *et al.* is certainly consistent with the present results, bearing a particular resemblance to $-\mathrm{Im}\{u\}$ of figure 1(*c*). The spanwise velocity fluctuations w exhibit similar behaviour, but Klebanoff *et al.* plot the *total* spanwise velocities in their figures 15 and 16, which includes the substantial mean flow resulting from the (Benney–Lin) longitudinal eddies. It is a remarkable, and unexplained, fact that their mean and fluctuating spanwise components almost cancel, once every cycle. The imaginary part of the spanwise fluctuation w for Hendriks' wave is shown in figure 1(*d*); the real part of w is virtually equal to $(\alpha/\gamma)\,\mathrm{Re}\,\hat{v}^{+}$. In order to model the total

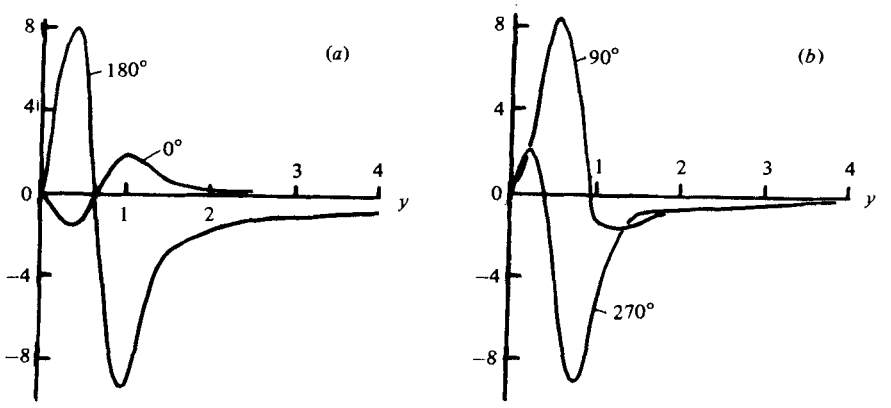

FIGURE 3. Instantaneous spanwise velocity profiles, $W + \mathrm{Re}\{we^{i\phi}\}$, $\phi = 0°$, 90°, 180° and 270°.

spanwise flow, we somewhat arbitrarily set the spanwise mean flow W equal to $\frac{2}{3}\,\mathrm{Im}\,(w)$. This choice was made after noting the similar form of $\mathrm{Im}\,(w)$ and Klebanoff *et al.*'s measured W. With a pair of oblique waves, and larger two-dimensional wave, the fluctuations and mean flow both vary roughly as $\cos\beta z$ in the spanwise direction (i.e. neglecting the 2β longitudinal eddy; cf. Klebanoff *et al.*, figure 18). Instantaneous profiles of $W + \mathrm{Re}\{we^{i\phi}\}$ ($\phi = \alpha_1 x - \omega t + \text{const.}$) at a fixed spanwise location are shown in figure 3 for $\phi = 0°$, 90°, 180° and 270°. These are in reasonable agreement with Klebanoff *et al.*'s figures 15 and 16 (cf. also Wortmann's 1977 figures 7 and 8).

An interesting observed feature is the apparently sudden change in the rate of phase increase with downstream distance, shown in figure 7 of Klebanoff *et al.* The gradient is constant up to about 5 in. downstream of the ribbon, indicating a fixed wavelength of 1·5 in. Thereafter, the gradient is again nearly constant for at least the next 4 in. (which extends beyond the appearance of the 'spike'), giving an increased wavelength of nearly 2 in. It may be argued that, up to 5 in., the two-dimensional wave is largest and beyond this point the three-dimensional waves are dominant. Therefore, since the three-dimensional waves have greater downstream wavelength, the observed wavelength is seen to increase. But such an explanation cannot account for the rather sudden change. Rather, some degree of 'spatial synchronization' by a nonlinear mechanism seems likely. However, the growth in boundary-layer thickness with downstream distance must also contribute to the observed change in wavelength.

Some remarks about the streamlines associated with three-dimensional waves are appropriate here. Firstly, it does not follow, as is often supposed, that the position of maximum downstream velocity u coincides with the 'crest of the wave' as indicated by the maximum streamline displacement. This is only true for two-dimensional waves. Secondly, the streamlines in the x'–y plane ($x' \equiv x - c_r t$) at a peak station $z = 0$ will have a structure different from that for a plane two-dimensional wave, even though $w = 0$ there. This is because $\partial w/\partial z$ is non-zero and the two-dimensional continuity equation is not satisfied. This has important repercussions for the shape of the streamlines near the critical layer. In general, they will not be the familiar 'Kelvin

cats'-eyes', even according to linear theory. The shape of the closed streamlines and the structure near the critical layer is strongly influenced by the relative phase of the x'- and y-velocity components (which is always 90° for two-dimensional waves). However, since such details are not as yet revealed by experiments, the matter is not pursued here.

3. 'Preferred' spanwise wavenumber

Klebanoff *et al.*'s experiments on natural transition, without any artificially introduced disturbance, reveal considerable similarities with those using the vibrating ribbon. The spanwise variation of a spontaneously growing disturbance is of course less regular than in the controlled experiments; but there again appears to be a preferred, or dominant, spanwise spacing of 'peaks' of around 1 in. (see their figure 33). It is unclear whether this 'preferred spacing' is evidence of a universal hydrodynamic phenomenon, or a feature of the particular experiment; but the former would not be too surprising.

The possibility of preferred spanwise wavenumbers was explored by Craik (1971) in his theory of resonant wave triads. As mentioned in § 2, the controlled experiments of Klebanoff *et al.* show no evidence of subharmonic frequencies; consequently, there appears to be no significant resonant interaction involving the fundamental two-dimensional wave and an oblique wave pair. But Craik also pointed out the existence of a triad for which the two-dimensional wave has twice the frequency of the fundamental (see Craik 1971, p. 398 and figure 2): in which case the two oblique waves have the same frequency as the fundamental, as in the experiments.

A 'free' linear mode with twice the fundamental frequency does not have a wavelength twice that of the fundamental; it is about 10 % less than this for $\alpha = 0{\cdot}25$ at $R = 882$, for instance. A slightly nonlinear two-dimensional wave with (real) wavenumber and frequency (α, ω) will normally drive a second harmonic $(2\alpha, 2\omega)$ which is not a free linear mode. But when the 'driving terms' have the same frequency as, and a rather similar wavenumber to, that of a free mode, then that mode – though 'off resonance' – may develop a significant amplitude. If this is so in the experiments of Klebanoff *et al.*, where a second harmonic of up to 20 % of the fundamental is reported, then a resonance mechanism similar to that of Craik (1971) could account for the spontaneous growth of a particular oblique wave pair. Extension of the resonance theory to this case, incorporating four waves which interact quadratically, has recently been carried out by Nayfeh & Bozatli (1979). Using the method of multiple scales, they include imperfect resonance through wavenumber mismatch and also the influence of boundary-layer growth. However, resonance models of this kind are applicable only if the 'second harmonic' is close to a free linear mode.

Craik (1971, p. 411) pointed out that the imposed spanwise spacing of 1·0 inch in the experiments of Klebanoff *et al.* is close to that required for resonance at one of the two frequencies studied. It would be interesting to know whether similar experiments with *differently spaced* spanwise irregularities would yield similar results. This would cast more light on the relevance of the resonance theory and help determine whether, in fact, there is a genuine preferred spanwise wavenumber. It should be noted, too, that the linearly most unstable disturbance with fixed frequency is not necessarily two dimensional: thus, for certain frequencies, even linear theory may provide a mechanism

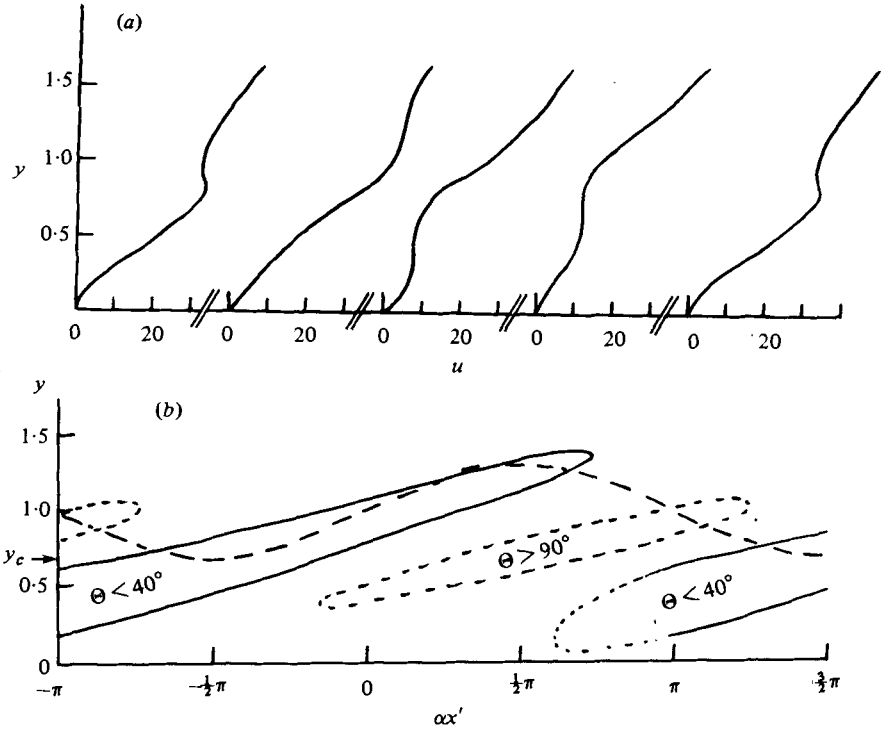

FIGURE 4. (*a*) Instantaneous u-velocity profiles for an oblique wave and uniform shear flow: $30y + \mathrm{Re}\{ue^{i\alpha x'}\}$, $0 \leqslant y < 1{\cdot}6$, at $\alpha x' = -\pi, \frac{1}{2}, 0, \frac{1}{2}\pi, \pi$. (*b*) Contours of constant shear denoting regions of enhanced shear with $\Theta \leqslant 40°$ and negative shear $\Theta > 90°$ for profiles shown in (*a*). The wavy dotted line shows an approximate streamline in the x'–y plane for a wave amplitude *half* that shown in (*a*).

for selecting a preferred spanwise wavenumber (I am grateful to Professor J. T. Stuart for emphasizing this point).

4. The high-shear layer

The appearance of the first high-frequency 'spike' is preceded by the development of a region of relatively high shear at some distance from the wall (see Tani 1969, p. 176). It is here shown that the vorticity perturbation associated with a linear two-dimensional wave does not display such a feature, but that for a pair of *oblique* waves yields instantaneous mean-flow profiles in broad agreement with those observed.

Figure 4(*a*) shows instantaneous profiles comprising oblique-wave fluctuation $\mathrm{Re}\,(ue^{i\alpha x'})$ (as shown in figure 1*c*) and a uniform mean flow $\bar{u} = 30y$. Of course, this is an oversimplification of the true situation, the actual mean flow being Blasius flow distorted by a secondary spanwise-varying component associated with the steady longitudinal-vortex structure. The intensity of this secondary steady flow is rather comparable to that of the fluctuations. The present profiles therefore model Blasius flow (which is approximately linear up to $y \simeq 1{\cdot}5$) and fluctuation but neglect the steady mean flow distortion.

It is seen that, in a reference frame travelling with the wave speed, regions of

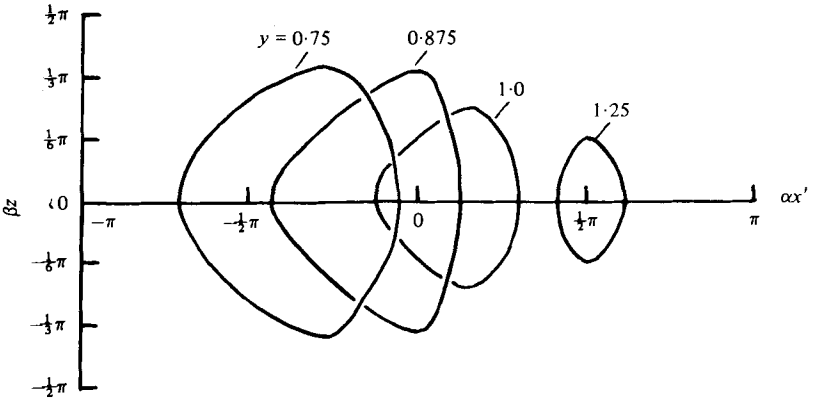

FIGURE 5. Contours of constant enhanced shear, $\Theta = 40°$, in x'–z plane for four fixed values of y (0·75, 0·875, 1·0 and 1·25).

enhanced shear propagate downstream and away from the wall and gradually decay as y increases beyond about 1·25. The velocity scale shown is arbitrary; but, to model Blasius flow with displacement thickness of unity, the constant free-stream velocity should be chosen equal to 53 units. The critical layer is then situated at $y = 0{\cdot}67$. Approximate contours of constant shear may be determined from the instantaneous profiles by considering the angle Θ, at various values of y, which the tangent to the profile makes with the u-axis. For each profile, values of y may be found at which the angle Θ takes a prescribed value. From these, contours such as those of figure 4(*b*) may be determined; those shown being for $\Theta = 40°$ (enhanced shear) and $\Theta = 90°$ (shear reduced to zero). To the order of approximation considered, the location of the enhanced shear region does not depend on wave amplitude, although the strength of the shear does. Accordingly, the contours of figure 4(*b*) also denote lines of constant shear for other wave amplitudes, a fact which is used later.

These results show a similarity with Kovasznay *et al.*'s figures 9 and 10. A similar propagation of the high-shear regions of *spanwise* velocity component is very evident in Wortmann's (1977) figures 7 and 8 and may also be deduced from Klebanoff *et al.*'s (1962) figure 16. This is entirely consistent with the present explanation that this feature is mainly due to the contribution from the $\hat{v}^{\pm}$ velocity components of the oblique waves. On the other hand, Wortmann's figure 6, showing 'Lissajous' figures' of the composite downstream and spanwise velocity vector over one wave period, is not in such clear agreement with linear theory. The latter predicts figures of elliptical or straight line shape, the axial directions of which are broadly in accord with Wortmann's data. The more complex shapes found by Wortmann may be due partly to the presence of higher harmonics owing to nonlinearity, but also to experimental scatter resulting from the indirect method of deducing velocities from bubble photographs and to an unexplained lack of symmetry in the data.

If the profiles shown in figure 4(*a*) are taken to correspond to a peak station $z = 0$, where two oblique waves reinforce each other (with the two-dimensional wave neglected) the intensity of u fluctuations varies as $\cos\beta z$. The maximum shearing rate is thereby reduced at 'off-peak' locations. Such x'–z dependence, at various fixed heights y, is shown in figure 5 as contours of constant enhanced shear, $\Theta = 40°$ for $y = 0{\cdot}75$, 0·875 and 1·0.

The instantaneous u profiles and regions of enhanced shear are very different for a two-dimensional wave. For $u = 30y + \mathrm{Re}\{2\hat{u}\,e^{i\alpha x'}\}$ and $\hat{u}(y)$ as given in figure 1(*a*) (i.e. for a wave amplitude twice that of the oblique wave just discussed) regions of enhanced shear with $\Theta \leqslant 40°$ do not penetrate beyond $y = 0{\cdot}3$. There is *some* shear enhancement above the critical layer, each half-cycle, but much less than for an oblique wave of comparable amplitude. Also, this enhanced-shear region does not 'propagate' like that for an oblique wave.

The distorted mean flow at a 'peak' station has enhanced shear approximately in the region $0{\cdot}85 < y < 1{\cdot}2$ (cf. Klebanoff *et al.*, figure 23) but this increase decays to zero at side stations and becomes a shear defect at 'valleys'. The magnitude of this effect appears to be comparable to that discussed above and so cannot be omitted from a realistic model of the instantaneous velocity profiles. The shapes of constant-shear surfaces in x'–y–z space (in a reference frame moving with the wave) become complicated when two- and three-dimensional waves and the mean-flow distortion are all included. The relative amplitudes and phases of the waves cause the shapes to change, and a detailed study is best delayed until precise numerical solutions are available corresponding to actual experimental waves and mean flow distortion. But, even at this stage, the qualitative picture seems clear.

The shear enhancement at peak stations is particularly large in the region near the edge of the boundary layer where the mean flow distortion and the three-dimensional wave fluctuation reinforce each other. The direct contribution of the two-dimensional wave in this region may be quite small; but it still plays an important, though indirect, role since the mean-flow distortion derives from the interaction of the two- and three-dimensional waves. The enhanced shear region is concentrated near peak stations, since both the mean flow distortion and three-dimensional wave contribution decay approximately to zero at 'side' stations. Figure 4(*b*) indicates that the region is inclined to the wall roughly at the angle $\tan^{-1}(\delta/\lambda)$, where δ is the displacement thickness and λ the wavelength; but it will eventually decrease in strength as the edge of the boundary layer is reached. Preliminary calculations using Hendriks' data give hope that the 'swept-back delta-wing' contours of greatest shear found by Kovasznay *et al.* (figure 11) may be modelled, to reasonable accuracy, by *linear* waves superimposed on the distorted mean flow. Since the mean flow distortion may itself be calculated by weakly nonlinear theory, it seems that weakly nonlinear theory may provide a satisfactory local description of the flow virtually up to breakdown. Confirmation by detailed computations is a desirable next step.

The proposal that weakly nonlinear theory can describe conditions virtually up to breakdown deserves careful examination. It is probable that disturbances at any given location can be so represented by suitable choice of the various amplitudes of waves and mean flow modification, as was done above. But it is not yet clear whether a weakly nonlinear theory can adequately describe the variations in wave amplitudes with downstream distance. Weakly nonlinear *models* certainly reproduce various qualitative features of the observed flows; but formal mathematical justification for such models is usually lacking. Higher-order terms are *definitely* negligible compared with those retained only for marginally unstable waves of very small amplitude (see Stewartson & Stuart, 1971). At Reynolds numbers removed from that for linear neutral stability and for larger wave amplitudes, the range of approximate validity of any weakly nonlinear model is difficult to establish (see the remarks of Usher & Craik 1975, pp. 457–8).

5. The secondary instability

The 'warping' or 'wrinkling' of the high shear layer (see Kovasznay *et al.*, figure 10) has been attributed to a secondary instability with a characteristic downstream wavelength much smaller than that of the fundamental waves. The associated records of u fluctuations display one or more 'spikes' (Klebanoff *et al.*, figure 21). The wavelength of such spikes is typically of order one tenth that of the fundamental wave. Klebanoff *et al.* conjectured that the secondary instability is akin to other observed inflexional instabilities of shear layers. The local flow near the high-shear layer is three-dimensional, with substantial spanwise variations in shear and also changes in spanwise velocity which are responsible for vortex stretching. The resulting secondary instability is therefore also strongly three-dimensional, the 'wrinkle' of the high-shear layer being rapidly 'swept back' on either side of the peak location. Klebanoff *et al.* show some evidence that the first 'spike' is, even at this early stage, a manifestation of a discrete 'hairpin eddy': but see Hama & Nutant (1963) for an alternative description.

A similar secondary instability, occurring within a localized wave packet, is described by Gaster (1978). This appears as a smaller-scale packet which later exhibits a tertiary instability. The flow visualization experiments of Wortmann (1977) give yet another view of the complex events taking place. It may be surmised from these various studies that the secondary instability at first comprises a small number of wavelike disturbances, but that these waves quickly roll up, somewhat like Kelvin–Helmholtz billows, into discrete vortices with a strong three-dimensional structure.

An even remotely adequate theoretical description of this process is lacking, but some limited progress has been made in constructing theoretical models for the initial growth of secondary disturbances in the high shear layer. The following comments are inevitably more speculative than those expressed above.

Presuming, like Klebanoff *et al.*, that the secondary instability is associated with an inflexion point of the shear-layer profile, the propagation speed of the small-scale disturbance should be close to that of the fluid of the high-shear layer. This varies somewhat with downstream position, because the location of the high-shear layer varies within the boundary layer; but it certainly exceeds that of the fundamental wave whenever the high-shear layer lies above the critical layer – as it does when the 'spike' is observed.

In their model of secondary instability, Greenspan & Benney (1963) consider the stability of various two-dimensional, inviscid, periodically varying (quasi-) parallel flows. For a model chosen to represent the velocity profile just prior to breakdown, they obtain the encouraging result that there is indeed a rapid instability with preferred wavenumber of about five times that of a primary two-dimensional wave. However, they rightly emphasize the crudity of their representation of the actual strongly three-dimensional shear layer.

As well as omitting spanwise variations, they also neglect the streamwise variations of the velocity profile. But, for constant amplitude three-dimensional waves, the enhanced shear layer moves away from the wall as it travels downstream, as described above, and there is no reference frame in which the velocity distribution is a function of time alone. In the experiments, the primary wave amplitudes also grow rather rapidly with downstream distance.

With an enhanced shear layer inclined like that indicated in figure 4(*b*), individual

fluid particles may spend a relatively short time in passing through the high-shear region. This is certainly so for small-amplitude waves; and strong secondary inflexional instability of the high-shear layer then seems unlikely. (Particles travelling at near the fundamental wave speed are located near the critical layer, which is not within the enhanced-shear region.) However, for larger waves, the streamlines may be displaced sufficiently to ensure that fluid particles spend longer in the high-shear region.

To demonstrate this, an approximate streamline is shown in figure 4(*b*) for a wave amplitude just half that which gives rise to the profiles of figure 4(*a*). (Recall that, although the strength of the enhanced shear region varies with wave amplitude, its location does not, to linear approximation.) The streamline displacement η from the mean level $y = 1{\cdot}0$ was calculated from the formula

$$d\eta/dx' = \tfrac{1}{2}\mathrm{Re}\{w e^{i\alpha x'}\}/(30y - 20)$$

with $w(y)$ as given by Hendriks' figure 2(*a*) (see appendix to Usher & Craik 1975). Though inaccurate near the critical layer, this formula is good enough for present purposes. It is seen that the streamline and the high-shear region are 'matched' for about $\frac{3}{4}$ of the fundamental wavelength. In contrast, the greater wave amplitude corresponding to the profiles of figure 4(*a*) is too large for such matching. Also, for smaller amplitudes, matching does not occur and, in addition, the maximum shear rate is reduced. It may be conjectured that, as the wave amplitude increases to that typical of the development of the 'spike', the combined effects of increased shear and the matching of shear layer and streamlines will favour the growth of secondary instability. In this case, the enhanced shear layer, observed relative to *streamline* coordinates, extends over a distance of $\frac{3}{4}$ of a fundamental wavelength and inflexional instability of this layer is very plausible. Small-scale disturbances should then attain maximum amplitude at about the point where the fundamental streamlines leave the high-shear layer. When both two- and three-dimensional waves are present, it is the streamline of the composite disturbance which must be matched to the high shear region: the particular example treated above should be regarded as an instructive oversimplification. Of course, the idea that the 'spike' results from warping of the high-shear layer is not new. But the likely importance of 'matching' of shear layer and streamlines has not previously been noted. Indeed, the familiar diagram of constant velocity contours and high-shear layer (see Tani 1969, figure 6) is easily misinterpreted as showing streamlines, which it does not.

Finally, it is appropriate to consider the theoretical model of breakdown proposed by Landahl (1972). A small-scale secondary wave riding on a large-scale primary wave pattern is assumed to evolve according to kinematic wave theory. It is claimed that a self-excited secondary wave attains large amplitude on the primary wave crest, because of space–time focusing, when its local group velocity is close to the phase velocity of the primary wave. This seems an attractive model, especially as the secondary waves can evolve in a truly nonlinear fashion. However, the applicability of conservative, or nearly conservative (see Jimenez & Whitham 1976), kinematic-wave theory to this problem has not been firmly established: for some objections, see Stewartson (1974). For other reasons, too, it is hard to accept Landahl's claims that his theory yields 'good quantitative agreement with the experiments...for the critical condition leading to breakdown' and that it can 'explain all the main qualitative breakdown features observed by Klebanoff *et al.* and others'.

Landahl calculated the complex phase velocity, say $c(\alpha_1)$, of secondary two-dimensional waves of local wavenumber α_1 on quasi-steady flows chosen to fit the instantaneous velocity profiles at 'wave crests' for Klebanoff *et al.*'s stations C and D. His results for station D, which is near to breakdown, show that the group velocity $\partial(\alpha_1 c)/\partial\alpha_1$, and also c itself, at the largest locally unstable wavenumbers α_1 are close to the phase velocity of the primary wave. No such agreement occurs at station C, where the group velocity associated with the 'wave-crest' profile is greater than the primary phase velocity. It is tempting to interpret this as support for the kinematic-wave model of breakdown. But such hopes are misplaced.

To quite good approximation, the phase and group velocities of the shorter unstable waves at stations C and D must agree with the flow velocities at the outer inflexion point of the respective instantaneous profiles. This is what one would expect from inviscid theory for an unstable shear layer. But the instantaneous profiles vary greatly over a single wave period in the manner described above. At fixed locations, the inflexion point moves towards the wall as the wave goes past (cf. figure 4 and Kovasznay *et al.*'s figure 9) with the instantaneous 'wave-crest' profiles examined by Landahl having inflexion points at (nearly) the largest values of y. (But see the remark at the end of § 2 regarding the dangers of equating maximum and minimum horizontal velocity fluctuations with crests and troughs of streamlines.) As the inflexion point moves towards the wall, the local phase and group velocities of short inflexionally unstable waves will decrease roughly according to quasi-steady theory. In particular, they will become less than Landahl's 'wave-crest' values; and it seems certain that there will be some moment during the wave cycle at which the group velocity of the short waves will equal the primary phase velocity for *each* point between C and D; and, indeed, for points upstream of C and downstream of D as well. Accordingly, no particular significance should be attached to the agreement of group velocity and primary phase velocity found by Landahl at station D.

In short, Landahl is wrong in assuming that the lowest group velocity occurs at the wave 'crest': instead, it is likely to be nearly the highest! In fairness, though, it should be said that his assumption may be roughly true for two-dimensional waves, since for these the inflexion point does not migrate through the boundary layer. But in the experiments of Klebanoff *et al.* and Kovasznay *et al.* the waves are strongly three dimensional.

Despite these criticisms, a kinematic-wave approach to the secondary instability may yet prove fruitful. But such a theory should be based on streamline co-ordinates for the primary flow, viewed in the reference frame of the primary wave pattern, and must accurately incorporate the structure of the evolving velocity profile. For short waves, presumably centred more or less on the path traced out by the inflexion point of the velocity profiles, the primary flow may indeed appear to be 'slowly-varying' in those regions where the streamlines and high-shear layer are roughly coincident, as discussed above. In this case, a kinematic-wave theory might be appropriate.

6. Conclusions

Many observed features of the nonlinear instability of the Blasius boundary layer are shown to be consistent with *three-dimensional* linear or weakly nonlinear theories, even as breakdown is approached. Particular attention is drawn to the 'propagating'

nature of the high-shear layer associated with three-dimensional waves. The results underline the need to guard against 'two-dimensional thinking', since the observed features cannot be explained in terms of 'locally two-dimensional' waves. It is suggested that the development of secondary instability is encouraged when the primary streamlines are sufficiently distorted to lie within the high-shear layer for most of a fundamental wavelength. Detailed computations based on existing theories, and an improved theory for the secondary instability, are still required to model the transition process to greater accuracy.

I am grateful to Professor Mark Morkovin both for letting me see his recent review article, prior to publication, and for detailed and instructive criticism of the first draft of this work; also to Dr Philip Morris for news of the work of Kachanov *et al.*, and to Professor J. T. Stuart for some comments.

REFERENCES

ANTAR, B. N. & COLLINS, F. G. 1975 *Phys. Fluids* **18**, 289–297.

BENNEY, D. J. 1961 *J. Fluid Mech.* **10**, 209–236.

BENNEY, D. J. 1964 *Phys. Fluids* **7**, 319–326.

BENNEY, D. J. & LIN, C. C. 1960 *Phys. Fluids* **3**, 656–657.

BOUTHIER, M. 1972 *J. Méc.* **11**, 599–621.

BOUTHIER, M. 1973 *J. Méc.* **12**, 76–95.

CORNER, D., HOUSTON, D. J. R. & ROSS, M. A. S. 1976 *J. Fluid Mech.* **77**, 81–103.

CRAIK, A. D. D. 1971 *J. Fluid Mech.* **50**, 393–413.

CRAIK, A. D. D. 1979 *Proc. IUTAM Symp. on Laminar-Turbulent Transition, Stuttgart.* Springer.

CROW, S. C. 1966 *J. Fluid Mech.* **24**, 153–164.

FASEL, H. 1976 *J. Fluid Mech.* **78**, 355–383.

GASTER, M. 1974 *J. Fluid Mech.* **66**, 465–480.

GASTER, M. 1975 *Proc. Roy. Soc.* A **347**, 271–289.

GASTER, M. 1978 Paper presented at 12th Symp. Naval Hydrodyn. Washington D.C.

GASTER, M. & GRANT, I. 1975 *Proc. Roy. Soc.* A **347**, 253–269.

GREENSPAN, H. P. & BENNEY, D. J. 1963 *J. Fluid Mech.* **15**, 133–153.

HAMA, F. & NUTANT, J. 1963 *Proc.* 1963 *Heat Transfer and Fluid Mech. Inst.* pp. 77–93. Stanford University Press.

HERBERT, T. 1975 *Proc. 4th Int. Conf. on Numerical Methods in Fluid Dynamics*, Lecture notes in Physics, vol. 35, pp. 212–217. Springer.

HERBERT, T. 1977 *Proc. AGARD Conf. No.* 224, *Copenhagen*, paper no. 3.

HOLSTEIN, H. 1950 *Z. angew. Math. Mech.* **30**, 25–49.

ITOH, N. 1974 *Trans. Japan Soc. Aero. Space Sci.* **17**, 175–186.

ITOH, N. 1977 *J. Fluid Mech.* **82**, 455–468.

JIMENEZ, J. & WHITHAM, G. B. 1976 *Proc. Roy. Soc.* A **439**, 277–287.

JORDINSON, R. 1971 *Phys. Fluids* **14**, 2535–2537.

JOSEPH, D. D. & HUNG, W. 1971 *Arch. Rat. Mech. Anal.* **44**, 1–22.

KACHANOV, Y. S., KOZLOV, V. V. & LEVCHENKO, V. Y. 1977 *Fluid Dynamics* **3–4**, 383–390 (translation of *Izv. Akad. Nauk S.S.S.R., Mekh. Zhid. i Gaza.* **3**, 49–58.

KACHANOV, Y. S., KOZLOV, V. V. & LEVCHENKO, V. Y. 1978 *A.I.A.A. Paper* no. 78–1131; *11th Fluid and Plasma Dynamics Conf. Seattle, Washington.*

KLEBANOFF, P. S. & TIDSTROM, K. D. 1959 *N.A.S.A. Tech. Note* D-195.

KLEBANOFF, P. S., TIDSTROM, K. D. & SARGENT, L. M. 1962 *J. Fluid Mech.* **12**, 1–34.

KOMODA, H. 1967 *Phys. Fluids* Suppl. **10**, S87–94.

KOVASZNAY, L. S. G., KOMODA, N. & VASUDEVA, B. R. 1962 *Proc. 1962 Heat Transfer and Fluid Mech. Inst.*, pp. 1–26. Stanford University Press.

LANDAHL, M. T. 1972 *J. Fluid Mech.* **56**, 775–802.

LANDAU, L. 1944 *C. R. Acad. Sci. U.R.S.S.* **44**, 311–314.

MACK, L. M. 1976 *J. Fluid Mech.* **73**, 497–520.

MACK, L. M. 1977 *Proc. AGARD Conf. No.* 224, *Copenhagen*, paper no. 1.

MACK, L. M. 1978 Paper presented at 12th Symp. Naval Hydrodyn., Washington, D.C.

MORKOVIN, M. V. 1978 *AGARDograph* AG–236.

MURDOCK, J. W. 1977 *A.I.A.A. J.* **15**, 1167–1173.

NAYFEH, A. H. 1979 Effect of streamwise vortices on Tollmien–Schlichting waves. Preprint.

NAYFEH, A. H. & BOZATLI, A. N. 1979 *A.I.A.A. 12th Fluid and Plasma Dyn. Conf. Williamsburg, Virginia*, paper 79–1496.

NELSON, G. & CRAIK, A. D. D. 1977 *Phys. Fluids* **20**, 698–700.

ORSZAG, S. A. 1976 *Proc. 5th Int. Conf. on Numerical Methods in Fluid Dynamics*, Lecture notes in Physics, vol. 59, pp. 32–51. Springer.

RAETZ, G. S. 1959 *Norair Rep.* NOR-59-383. Hawthorne, Calif.

RESHOTKO, E. 1976 *Ann. Rev. Fluid Mech.* **8**, 311–349.

ROSS, J. A., BARNES, F. H., BURNS, J. G. & ROSS, M. A. S. 1970 *J. Fluid Mech.* **43**, 819–832.

SARIC, W. S. & NAYFEH, A. H. 1975 *Phys. Fluids* **18**, 945–950.

SARIC, W. S. & REYNOLDS, G. A. 1979 *Proc. IUTAM Symp. on Laminar–Turbulent Transition, Stuttgart.* Springer.

SCHUBAUER, G. B. & SKRAMSTAD, H. K. 1948 *N.A.C.A. Rep.* no. 909.

STEWARTSON, K. 1974 *Polish Acad. Sci. Fluid Dyn. Trans.* **7**, 101–128.

STEWARTSON, K. & STUART, J. T. 1971 *J. Fluid Mech.* **48**, 529–545.

STUART, J. T. 1960 *J. Fluid Mech.* **9**, 353–370.

STUART, J. T. 1962 *Adv. Aero. Sci.* **3**, 121–142.

TANI, I. 1969 *Ann. Rev. Fluid Mech.* **1**, 169–196.

USHER, J. R. & CRAIK, A. D. D. 1975 *J. Fluid Mech.* **70**, 437–461. (Appendix by F. Hendriks.)

WATSON, J. 1960 *J. Fluid Mech.* **9**, 371–389.

WORTMANN, F. X. 1977 *Proc. AGARD Conf. No.* 224, Copenhagen, paper no. 12.

WYGNANSKI, I., HARITONIDIS, J. H. & KAPLAN, R. E. 1979 *J. Fluid Mech.* **92**, 505–528.